APAE MEMO NO. 107

Copy No. 6

COMPARISON OF PREDICTED AND ACTUAL CONTROL ROD DROP TIME FOLLOWING SCRAM OF THE APPR-1

Contract No. AT(11-1)-318

Issued July 12, 1957

Author- J.O. Brondel

ALCO PRODUCTS, INC.
P.O. Box 414
Schenectady, N.Y.

DISCLAIMER

DISTRIBUTION

External:

Copies	
1	U.S. Atomic Energy Commission Schenectady Operations Office P.O. Box 1069 Schenectady, N.Y. Attention: Capt. J.F. Smith, Jr.
2-5	U.S. Atomic Energy Commission 1901 Constitution Avenue Washington 25, D.C. Attention: Classified Technical Library for J.P. Lampert
6-25	U.S. Atomic Energy Commission Reference Branch, Technical Information Service Extension P.O. Box 62 Oak Ridge, Tenn. Attention: M. Day
26-27	Nuclear Power Branch Engineer Research & Development Laboratories Fort Belvoir, Virginia Attention: Major J.A. Bacci
28-29	Union Carbide Nuclear Company Oak Ridge National Laboratory X-10 Laboratory Records Department P.O. Box "P" Oak Ridge, Tenn.

Internal:

30-47	Alco Products, Inc. P.O. Box 414 Schenectady, N.Y.	
	K.Kasschau	J.P.Tully
	J.F.Haines	T.F.Connolly
	H.L.Weinberg	W.Waddell
	J.L.Meem	S.M.Ingeneri
	W.M.S.Richards	J.O.Brondel
	J.G.Gallagher	7- File

TABLE OF CONTENTS

I SUMMARY

A detailed analysis of hydraulic and mechanical forces affecting control rod drop time has been made to determine a mathematical expression for rod position in terms of elapsed time after initiation of a scram. The elapsed time analyzed in this report is exclusive of the instrument delay and clutch decay intervals.

A comparison of predicted rod drop to actual field measurement (Figs. 1 and 2) shows good agreement both with and without primary loop flow.

II INTRODUCTION

During the initial design stage of the APPR-1, a calculation was made of the approximate control rod drop rate at scram. The method used was necessarily "rough" since much of the detailed information required for a more exact approach was not yet available. Hydraulic drag forces were not considered for this reason and in the belief that they would not be very significant in the design contemplated. The predicted rod acceleration rate was 3/4 g.

Upon completion of initial designs for the control rod and drive mechanisms, an experimental model and test rig were assembled at ALCO. Drop acceleration rates with simulated primary loop flow measured about 0.6 g.

Following these tests, the core orificing program employing full flow tailoring was adopted. Core pressure drop, and therefore hydraulic drag forces on the rods were greatly increased. The final rod drive mechanism adopted has a greater angular moment of inertia restraining rod drop, thus a further decrease in the rod drop rate should be expected.

Upon completion of APPR-1 construction at Ft. Belvoir, field tests were made of the actual control rod drop rates. These tests showed an acceleration rate of 0.4 g at scram with rated primary loop flow. As this drop rate differs greatly from that originally estimated, the purpose of this memo is to re-examine, in the much greater detail now possible, the drop time to be expected based on a thorough analytical study.

It should be emphasized that the lower rod acceleration rate of about 0.4 g is completely satisfactory for safe reactor operation. APAE Memo No. 97 analyzes the effect of this reduced acceleration on a startup accident, potentially the most dangerous. The conclusion reached is that the reduced acceleration rate does not constitute any significant increase in energy release, the maximum release being far below that required to cause melting at the fuel element center line.

III FORCES AND MASSES AFFECTING DROP RATE

1. Weight of control rod 72 lb.

2. Buoyancy - The buoyant force on the submerged rod is determined by the weight of the displaced water at operating conditions:

$$\frac{(72 \text{ lb metal})}{(0.286 \text{ lb/in}^3\text{metal})(0.0193 \text{ ft}^3/\text{lb water})(1728 \text{ in}^3/\text{ft}^3)} = 7.6 \text{ lb}$$

3. Equivalent mass of rod drive - After the magnetic clutch of the control rod drive mechanism is disengaged by the scram signal, some of the rotating parts remain geared to the rod. Their angular moment of inertia can be converted to an equivalent mass to be accelerated linearly by the rod. The relationship is determined by the torque arm, in this case the pitch radius of the pinion gear meshing with the rod rack, and is calculated as shown below:

$$F\,r = I\,\alpha \quad ; \quad \alpha = \frac{a}{r}$$

$$F = \frac{Ia}{r^2} \quad ; \quad F = \frac{w}{g}\,a$$

$$W = \frac{Ig}{r^2} = \frac{(.0015)(32.2)}{(1/12)^2} = \ldots\ldots \quad 7.0 \text{ lb.}$$

Where:

F	=	Force at pinion pitch radius,	lb
r	=	Pinion gear pitch radius,	ft
I	=	Angular moment of inertia,	slug - ft^2
α	=	Angular acceleration,	radians/sec^2

a = (Linear) rod acceleration, ft/sec^2

W = Equivalent weight, lbs.

4. Friction - The torque required to overcome the dynamic friction of the rotating parts mentioned in section III-3 is estimated at 10 lb-in. Since the torque arm or pinion pitch radius is 1 in, the equivalent friction force on the rod is.....10 lb.

5. Steady State hydraulic force - If a primary loop pump is in operation, a viscous drag force will be exerted upward on each rod by its internal and external water flow. The magnitude of this drag force is determined by the pressure drop along the rod, ignoring effects of elevation change. The resulting drop is due to flow alone. Including the elevation effect would include the buoyance force of Section III-2, which is more conveniently handled separately.

If flow velocities are moderate, as they are in the APPR-1 core, pressure changes due to changes in velocity magnitude or direction are negligible. For a simple pipe, the flow forces are determined as indicated below:

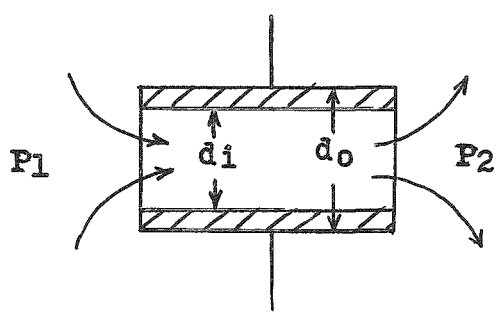

For steady state flow:

Viscous drag = $(P_1-P_2)\ \frac{\pi\, di^2}{4}$

Total flow force = $(P_1-P_2\ \frac{\pi\, do^2}{4}$

This same relationship can be applied to a control rod, even though the flow pattern is more complex. An example is shown below, neglecting flow outside the rod:

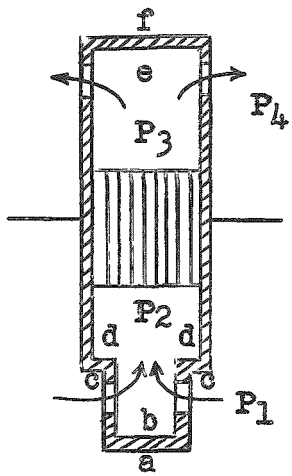

P = Pressure in areas as indicated

a,b,c,d,e,f = Areas of surfaces as indicated

Net upward flow force = $P_1(a + c) + (P_2-P_3)e + P_3e - P_2(b + d) - P_4f$

But $a + c = f$; $b + d = e$

Net upward flow force = $P_1f + P_2e - P_3e + P_3e - P_2e - P_4f = (P_1-P_4)f$

When flow outside the rod is also considered, the additional drag force is assumed to be applied equally to the inner and outer walls of the surrounding annular passage. As forces on the stationary fuel elements are not pertinent, only the half of the additional drag force applied to the control rod affects rod drop. Total rod flow force is derived below:

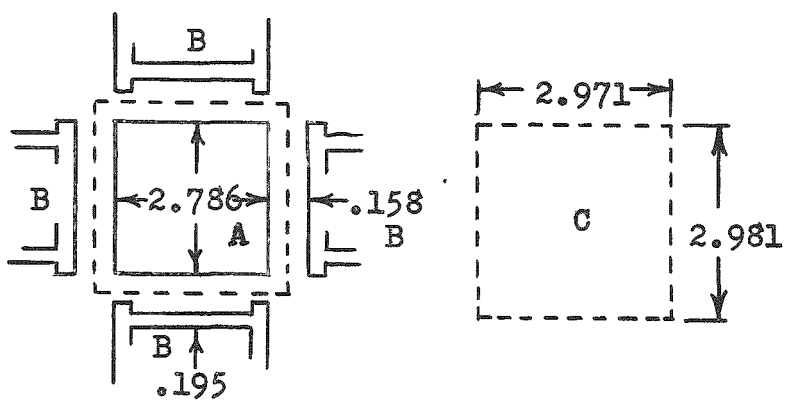

Pressure drop across core, neglecting elevation effects, is 1.75 psi.

A - Control rod cross-section

B - Stationary element cross-section

C - Equivalent rod cross-section for the flow force

Steady state flow force = (1.75 psi)(2.971 in)(2.981 in) = 15.5 lb.

6. Transient hydraulic forces - Resisting rod motion are hydraulic forces which vary generally as the square of the rod velocity. These forces are determined by viscous drag, stagnation pressure build-up, etc. and are difficult to define analytically. In the table below* are indicated drag coefficients for circular cylinders, which may be considered as resembling control rods:

$\frac{L}{D}$ Ratio	C_D	
0	1.12	Drag = $C_D\left(\frac{V^2}{2g}\right)\rho A$
1	0.91	
2	0.85	
4	0.87	
7	0.99	
[23]	[1.64]	Extrapolated

Circular Cylinders, axis parallel to flow, Reynolds No.$>10^3$

The increase in the drag coefficient between L/D ratios of 4 and 7 should be due only to the increased viscous drag corresponding to the increased length of cylinder. A linear extrapolation appears justified, yielding a coefficient of 1.64 for the L/D ratio of 23 corresponding to control rod minus its rack.

* Rouse, Hunter, "Elementary Mechanics of Fluids" p. 249, New York, John Wiley and Sons, 1946.

The effects of adding the rack, and especially that of confining the rod to drop through the small clearance of the core passage, would be an expected increase in the coefficient to a minimum of 2.0. Accordingly, this is the value used. Greater precision of determination is not felt necessary since the additional influence on control rod drop is very small compared with the effects of the other restraining forces considered.

$$\text{Transient drag force} = C_D\left(\frac{v^2}{2g}\right)\rho A$$

$$= \frac{(2.0)(2.786\ \text{in})^2 \quad v^2}{2g\ (.0193\ \text{ft}^3/\text{lb})(144\ \text{in}^2/\text{ft}^2)} = .087\, v^2\ \text{lb}$$

7. Trapped water - Drop time of the rod and restriction of flow are considered to validate the assumption that the water contained by the rod is essentially trapped and must be accelerated with the rod. The corresponding water weight is therefore added to the mass being accelerated but not to the accelerating force.

$$\text{Weight of trapped water} = \frac{0.187\ \text{ft}^3}{0.0193\ \text{ft}^3/\text{lb}} = \ldots\ldots\ldots\ 9.7\ \text{lb}$$

IV EQUATION OF ROD MOTION

$$F = M a$$

$$F_f - F_v V^2 = M \frac{dv}{dt} \qquad \left[\text{with primary loop flow}\right] \quad (1)$$

Eq. (1) is the basic differential equation defining the motion. In this form it is non-linear, and is therefore manipulated algebraically for easier solution:

$$\frac{dt}{dv} = \frac{M}{F_f - F_v V^2}$$

$$t = M \int \frac{d v}{F_f - F_v V^2} \quad ; \quad \int \frac{dx}{a - bx^2} = \frac{1}{2\sqrt{ab}} \ln \frac{\sqrt{ab} + bx}{\sqrt{ab} - bx} + c$$

where $a > o$, $b > o$

$$t = \frac{M}{2\sqrt{F_f F_v}} \ln \frac{\sqrt{F_f F_v} + F_v V}{\sqrt{F_f F_v} - F_v V} + C_1 \qquad (2)$$

Boundary condition: When $t = 0$, $v = 0$:

$$0 = \frac{M}{2\sqrt{F_f F_v}} (\ln 1 = 0) + C \quad ; \quad C_1 = 0$$

The solution for "t" in terms of "v" is then rewritten in terms of "$\frac{ds}{dt}$". If the reduction of order method were not used, and eq.(1) were written directly in terms of "s" the resulting non-linear equation could not be manipulated so easily.

$$t = \frac{M}{2\sqrt{F_f F_v}} \ln \frac{\sqrt{F_f F_v} + F_v \frac{ds}{dt}}{\sqrt{F_f F_v} - F_v \frac{ds}{dt}}$$

$$\ln \frac{\sqrt{F_f F_v} + F_v \frac{ds}{dt}}{\sqrt{F_f F_v} - F_v \frac{ds}{dt}} = \frac{2\sqrt{F_f F_v}\ t}{M}$$

$$\frac{\sqrt{F_f F_v} + F_v \frac{ds}{dt}}{\sqrt{F_f F_v} - F_v \frac{ds}{dt}} = e^{2\sqrt{F_f F_v}\, t/M} = e^{\alpha t}\,; \quad \alpha = \frac{2\sqrt{F_f F_v}}{M}$$

By algebraic rearrangement:

$$\frac{ds}{dt} = \frac{\sqrt{F_f F_v}}{F_v} \frac{(e^{\alpha t} - 1)}{(e^{\alpha t} + 1)}$$

$$s = \sqrt{\frac{F_f}{F_v}} \left[\int \frac{e^{\alpha t}\, dt}{e^{\alpha t} + 1} - \int \frac{dt}{e^{\alpha t} + 1} \right]$$

Since $\int \frac{e^{ax}\, dx}{b + ce^{ax}} = \frac{1}{ac} \ln\left(b + ce^{ax}\right)$; $\int \frac{dx}{b + ce^{ax}} = \frac{x}{b} - \frac{1}{ab} \ln(b + ce^{ax})$

$$s = \sqrt{\frac{F_f}{F_v}} \left[\frac{1}{\alpha} \ln\left(e^{\alpha t} + 1\right) - t + \frac{1}{\alpha} \ln\left(e^{\alpha t} + 1\right) \right]$$

$$s = \frac{M}{F_v} \left[\ln\left(e^{\alpha t} + 1\right) - \frac{\alpha t}{2} + C_2 \right]$$

Boundary condition: when $t = 0$, $s = 0$:

$$0 = \frac{M}{F_v} \left[\ln 2 - 0 + C_2 \right]; \quad C_2 = \ln 2$$

The final solution for rod travel "s" vs. time "t" is then:

$$s = \frac{M}{F_v} \left[\ln\left(e^{2\sqrt{F_f F_v}\, t/M} + 1 \right) - \sqrt{\frac{F_f F_v}{M}}\, t - \ln 2 \right] \quad (3)$$

Symbols:

a - Acceleration of rod, ft/sec^2

C - Constant of integration

F_f - Fixed force acting on rod, lb

F_v - Variable force acting on rod, lb/v^2

M - Mass being accelerated, slugs

s - Travel of rod, ft

t - Elapsed time, sec.

V - Velocity of rod, ft/sec.

V PREDICTED VS. ACTUAL ROD DROP RATES

Control rod drop rate measurements were made at the site of the APPR-1 both with and without a primary loop pump running. Only the steady state drag force is considered to be affected by this change.

The substitution of numerical values for the variables in eq. (3) of Section IV is as follows, with numerical subscripts referring to descriptive paragraphs in Section III:

$$s = \frac{M}{F_v}\left[\ln\left(e^{2\sqrt{F_f F_v}\, t/M} + 1\right) - \frac{\sqrt{F_f F_v}}{M}\, t - \ln 2\right]$$

$$M = \frac{W_1 + W_3 + W_7}{g} = \frac{72.0 + 7.0 + 9.7}{g} = 2.76 \text{ slugs}$$

$$F_f = F_1 - F_2 - F_4 - F_5 = 72.0 - 7.6 - 10.0 - 15.5 = 38.9 \text{ lb with flow}$$

$$F_f = F_1 - F_2 - F_4 = 72.0 - 7.6 - 10.0 = 54.4 \text{ lb without flow}$$

$$F_v = F_6 = 0.087 \text{ lb-sec/ft}$$

$$s = 31.7\left[\ln\left(e^{1.33\, t} + 1\right) - 0.666\, t - 0.693\right] \text{ ft with primary flow}$$

$$s = 31.7\left[\ln\left(e^{1.58\, t} + 1\right) - 0.788\, t - 0.693\right] \text{ ft without primary flow}$$

As further check on the analytical approach used, the predicted drop rate is compared with that measured in previous experiments with an earlier model of the APPR-1 rod drive mechanism.

W_3 = 5.3 lb. equivalent mass of rotating parts

F_4 = 7.5 lb. equivalent friction force

F_5 = 7.4 lb. steady state hydraulic drag

$$s = 31.0\left[\ln\left(e^{1.54\,t} + 1\right) - 0.769\,t - 0.693\right] \text{ ft with flow}$$

$$s = 31.0\left[\ln\left(e^{1.65\,t} + 1\right) - 0.824\,t - 0.693\right] \text{ ft without flow}$$

The previously derived equations of predicted drop distance vs. elapsed time are compared graphically with actual drop measurements in Figs. 1 through 3 as follows:

Fig. 1 - With loop flow, Ft. Belvoir tests

Fig. 2 - Without loop flow, Ft. Belvoir tests

Fig. 3 - With simulated loop flow, early model of drives.

Fig. 4 - Without simulated loop flow, early model of drives.

Actual control rod motion is not initiated until the field of the magnetic clutch has decayed sufficiently to permit slip. This instant, taken as zero time in the graphs, is determined by visual examination of data from recording instruments. A reading error of several milliseconds is therefore possible. Also, since the first few milliseconds of rod travel is still being resisted by the decaying clutch torque, initial rod acceleration is reduced. These factors explain the initial spread of the experimentally determined drop curves.

All comparisons show good agreement between predicted and actual control rod drop time. It should be noted that only the first inch of rod drop at the very most is of immediate concern in scramming the reactor. As indicated by APAE Memo No. 97, the power level is already insignificant after a rod drop of about 0.3 inches.

Since the reactor could never approach criticality while the bottom ends of the control rod racks were still inserted in the dashpots, the very low acceleration rate attendant with a scram at this rod position is of no concern.

VI DROP TESTS ON MODIFIED EQUIPMENT

1. Modified Control Rod Cap

A special control rod cap was made, having a 1 3/4 inch diameter opening in the top to permit axial exit with reduced flow restriction. The expected effect of installing this cap was a slight increase in the rod acceleration at scram since there is less of a tendency for the water contained by the rod to be trapped and accelerated at the same rate. Steady hydraulic drag is unaffected since the decrease in core pressure drop is negligible.

As the special cap was necessarily about 9 1/2 lbs. lighter than the original cap it replaced, a second special cap was made without an opening but with the same weight as the first. A better comparison of drop tests was therefore possible to determine the "hole effect".

A comparison of site test results using the special rod caps showed a significant increase in acceleration rate with the axial opening. However, both curves are contained by the deviation band of Fig. 1, that for the closed cap being on the slower drop side of the band and that for the open cap being on the faster side. A more major variation of either special cap curve from the mean standard cap curve was not expected since the percent reduction in rod weight and in total flow restriction through the rod is not very great.

2. Shroud Around Upper Portion of Rod

Also investigated in the control rod drop tests was the possibility of binding of the rods due to lateral flow of the coolant in the upper plenum chamber. The arrangement of rods projecting up into this chamber is illustrated below:

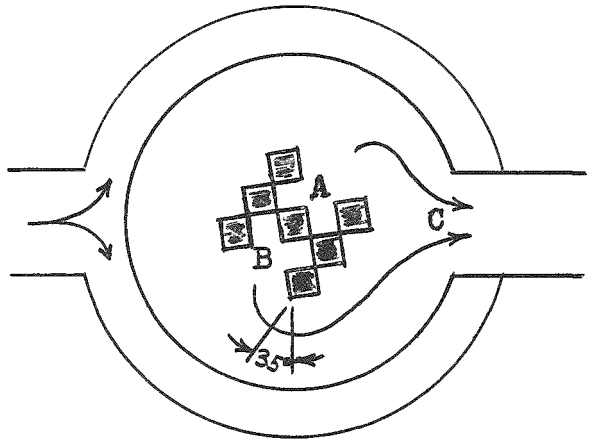

Top View of Reactor Vessel

Flow resistance along path A-C is less than along path B-C. A pressure differential could conceivably exist between areas A and B or C and B, causing a lateral thrust on the rods separating these areas sufficient to increase the friction and thereby reduce acceleration at scram.

Accordingly, a cylindrical shroud was placed around the control rod grouping to eliminate lateral flow and make the flow resistance along the paths more equal. Drop tests were then conducted, but no detectable shroud effect noted.

Concurrently, tests were performed on the APPR-1 air flow rig at ALCO with two objectives. The first was to determine by static pressure measurement if a significant thrust could exist.

The second objective was to determine the increase in primary pressure drop across the reactor vessel with a control rod shroud installed.

For the tests, all rods were raised to the normal safety rod position since this is approximately the maximum withdrawl that will ever be used in normal reactor operation. Pressure readings taken in regions A and B (see preceeding illustration) without the shroud showed negligible variations, thereby indicating no significant lateral rod thrusts possible. Testing with the cylindrical shroud installed showed that its use would increase the pressure drop across the reactor vessel by only about 1%. In terms of overall primary loop drop, this increase is only a few tenths of a percent.

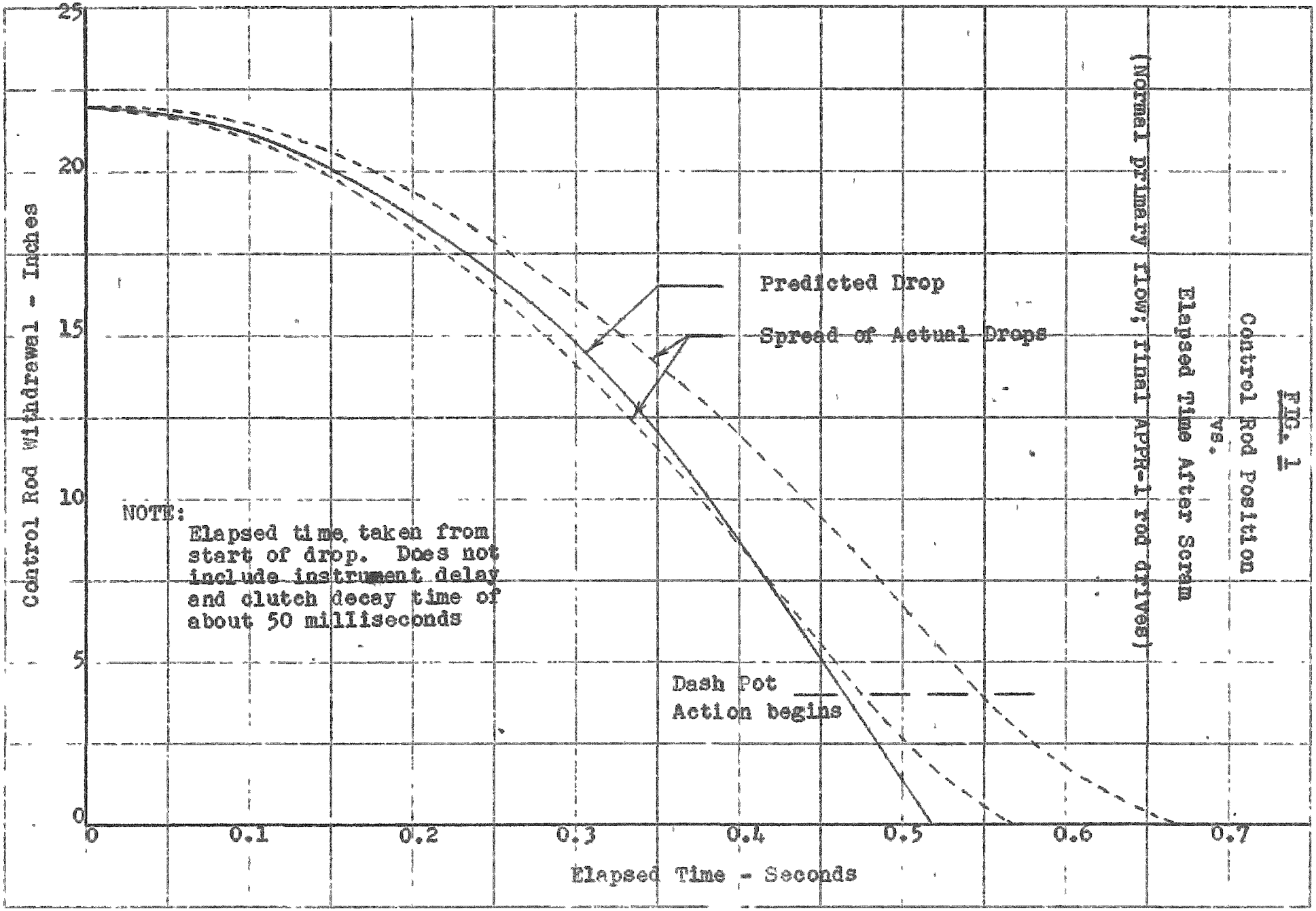

FIG. 1

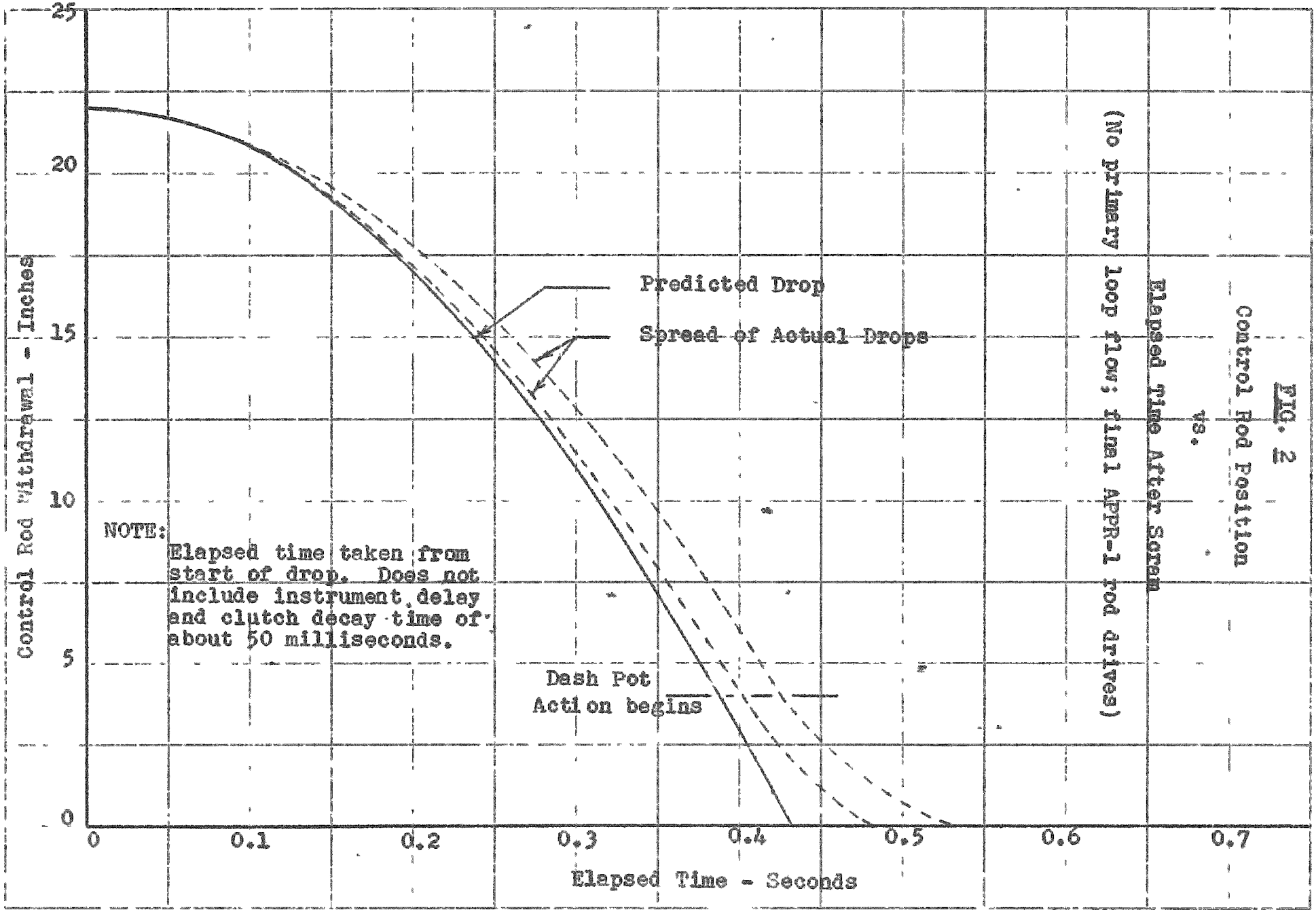

FIG. 2

Control Rod Position

vs.

Elapsed Time After Scram

(No primary loop flow; final APPR-1 rod drives)

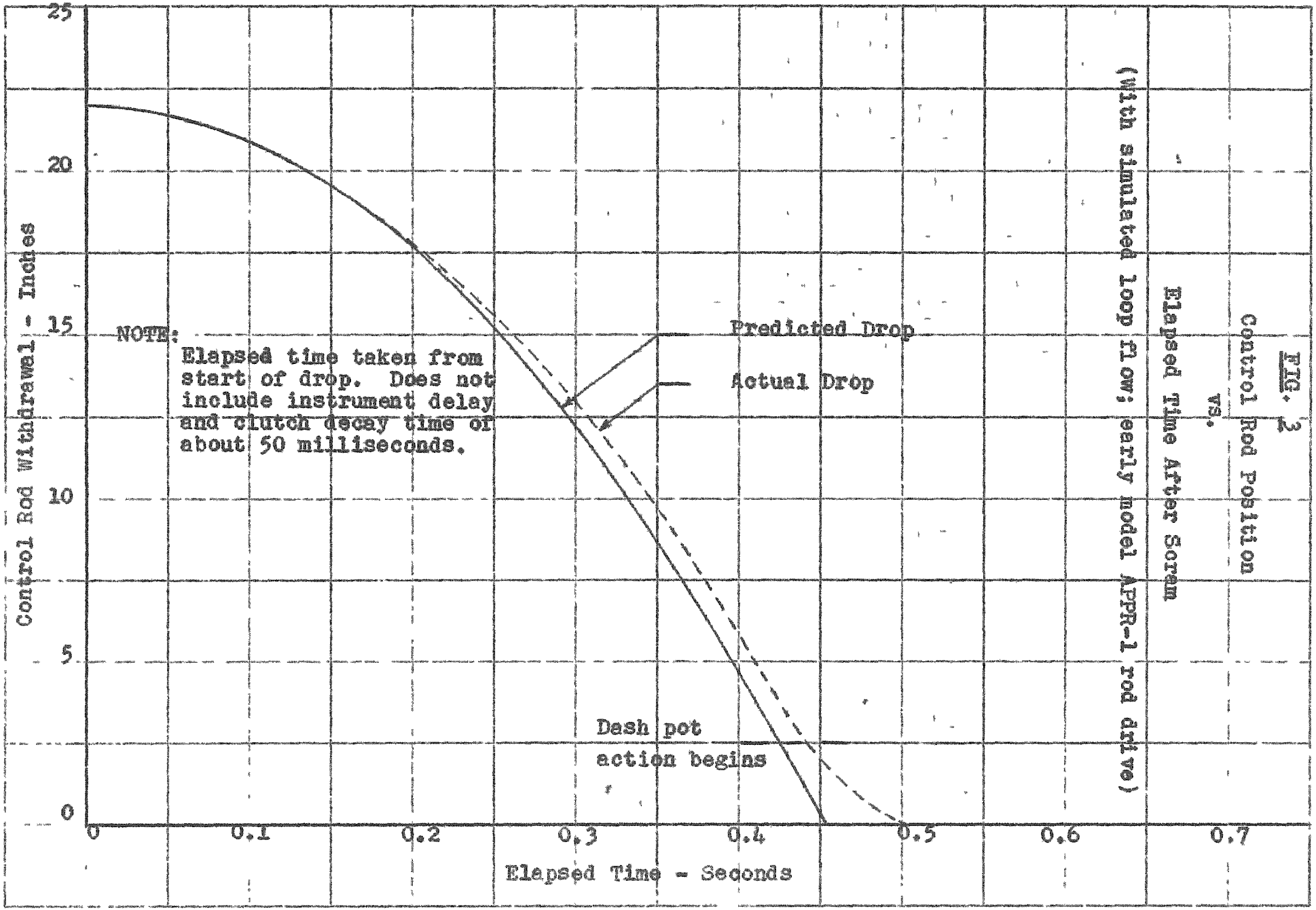

FIG. 3

Control Rod Position vs. Elapsed Time After Scram

(With simulated loop flow; early model APPR-1 rod drive)

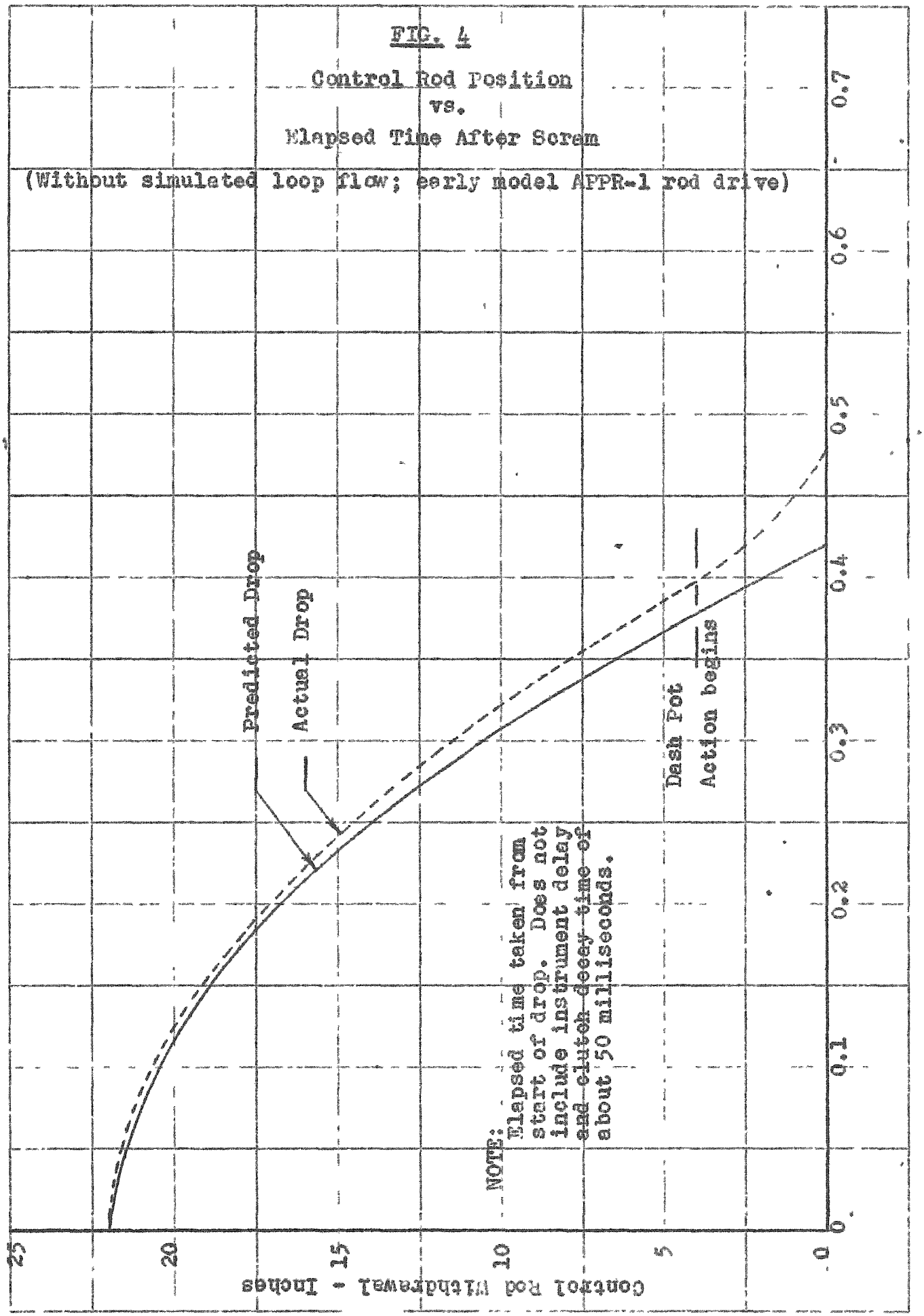

FIG. 4

Control Rod Position
vs.
Elapsed Time After Scram

(Without simulated loop flow; early model APPR-1 rod drive)